Thermal and Structural Stability of Adsorbed Proteins

Sumit Sharma,[†] B. J. Berne,[‡] and Sanat K. Kumar[†*]
[†]Department of Chemical Engineering and [‡]Department of Chemistry, Columbia University, New York, New York

ABSTRACT Experimental evidence suggests that proteins adsorbed to hydrophobic surfaces at low coverages are stabilized relative to the bulk. For larger coverages, proteins unfold and form β-sheets. We performed computer simulations on model proteins and found that: 1), For weakly adsorbing surfaces, unfolded conformations lose more entropy upon adsorption than folded ones. 2), The melting temperature, both in the bulk and at surfaces, decreases with increasing protein concentration because of favorable interprotein interactions. 3), Proteins in the bulk show large unfolding free energy barriers; this barrier decreases at stronger adsorbing surfaces. We conjecture that typical experimental temperatures appear to be below the bulk melting temperature for a single protein, but above the melting temperature for concentrated protein solutions. Purely thermodynamic factors then explain protein stabilization on adsorption at low concentrations. However, both thermodynamic and kinetic factors are important at higher concentrations. Thus, proteins in the bulk do not denature with increasing concentration due to large kinetic barriers, even though the aggregated state is thermodynamically preferred. However, they readily unfold upon adsorption, with the surface acting as a heterogeneous catalyst. The thermal behavior of proteins adsorbed to hydrophobic surfaces thus appears to follow behavior independent of their chemical specificity.

INTRODUCTION

The adsorption of proteins on hydrophobic surfaces is driven by the "hydrophobic effect" (1–3). Proteins adsorbed on hydrophobic surfaces show rich structural and thermodynamic behavior. Vermeer et al. (4), Norde and Giacomelli (5), Zoungrana et al. (6), and Mollmann et al. (7) have shown, via differential scanning calorimetry and circular dichroism studies, that at low adsorbed coverages (less than a monolayer), proteins are less susceptible to thermal denaturation. Presumably, unfolding occurs at higher temperatures, if at all. Most proteins do not lose intramolecular secondary structure upon adsorption to hydrophobic surfaces at low adsorbed concentrations (4–6,8–12) (see Table 1). To our knowledge, no theoretical work has been performed to understand the thermal stability of adsorbed proteins under these conditions, and work has been restricted to structural studies. Experimental studies at large adsorbed concentrations (monolayer or more) have shown an opposite trend. These proteins were reported to lose intramolecular secondary structure and gain intermolecular β-sheets and random coil content, implying that the proteins denature upon adsorption (9,13–15).

These experiments pose a variety of questions that we address theoretically here.

First, why is the folded structure of an isolated protein stabilized by a hydrophobic surface?

Second, why do increases in protein concentration change the nature of adsorbed conformations?

We have simulated both isolated model proteins and two protein molecules (as a mimic for concentration effects) near a hydrophobic surface. Our simulation results show that over a range of small to intermediate surface hydrophobicities, entropic effects dominate. Thus, it is easier to adsorb a folded conformation versus an unfolded conformation, and the melting temperature of the protein is shifted upward, as found in experiments. Clearly, thermal stability is coupled to enhanced structural stability of the folded state. Simulation results of two protein molecules show that they become destabilized as their concentration increases. However, because of the presence of large unfolding free energy barriers in the bulk, the proteins do not spontaneously unfold and denature. The presence of a hydrophobic surface brings down the unfolding free energy barriers, explaining why proteins, present in the folded state in the bulk, denature upon adsorption at high surface concentrations.

MATERIALS AND METHODS

We use the method of Dill (16), i.e., hydrophobic (H)-polar (P) (two-letter) lattice-based implicit solvent modeling, for modeling our proteins. In the HP lattice model, a protein is represented as a cubic lattice chain of two types of beads: H and P. The surface is modeled as a two-dimensional impenetrable plane with a two-dimensional lattice commensurate with the three-dimensional lattice in which the protein resides. Because the model does not account for solvent molecules, we incorporate the hydrophobic interactions between two H moieties on a chain, and the interaction between an H monomer and a hydrophobic surface through the use of energetic interactions. The energy of interaction between any two nonbonded H beads, $\varepsilon_{\text{H-H}}(r)$, is -1 (in arbitrary energy units) when the interbead distance, $r = 1$ lattice unit, and is zero when $r > 1$. All other interactions ($\varepsilon_{\text{H-P}}(r)$, $\varepsilon_{\text{P-P}}(r)$, $\varepsilon_{\text{H-solvent}}(r)$, $\varepsilon_{\text{P-solvent}}(r)$, and $\varepsilon_{\text{solvent-solvent}}(r)$) are set to zero for all r. We characterize the ratio of the energy of a surface-H interaction to the energy of a pair of H contacts by λ_s. ($\lambda_s = 1$ implies that the surface hydrophobicity matches that of intrachain H-H contacts.) Hence, the energy of interaction between an H bead of the protein and the surface is equal to $\lambda_s\,\varepsilon_{\text{H-s}}$, where $\varepsilon_{\text{H-s}}(r)$ is -1 when $r = 1$, and zero otherwise.

Here we note that lattice protein models lose the atomistic details of the side chains and the protein backbone, which may influence the free

Submitted March 3, 2010, and accepted for publication May 5, 2010.

*Correspondence: sk2794@columbia.edu

Editor: Gerhard Hummer.

0006-3495/10/08/1157/9 $2.00

doi: 10.1016/j.bpj.2010.05.030

TABLE 1 Thermodynamic properties, thermal stability, and changes in the secondary structure upon adsorption to Teflon particles of different proteins as reported in the literature

	M_o (kDa)	T_m (k)	ΔH_d (kJ/mol)	ΔG_d (kJ/mol)	Thermal stability upon ads	Fractional surface coverage	Change in secondary structure on adsorption to Teflon
Fab	50	334	935	101	Increases	0.3	Increases (4)
Fc	50	344	900	120	Increases	0.3	Increases (4)
BSA	68	330	748	72	Increases	0.15–0.4	Increases (5)
Cutinase	20	326	608	52	Increases	0.2	Decreases (6)
Chym	25	322	510	38	Increases	0.4	Increases (6)
Lys	14	346	420	58	Increases	0.2–0.5	Increases (5)
Savinase	—	—	—	—	—	0.25	Increases (12)
Amyloid β-peptide	4.3	—	—	—	—	0.25	Increases (8)

Fractional surface coverages were calculated by assuming adsorbed proteins' dimensions equal to that of the native state with "flat-on" orientation.

energy landscape of a protein. For example, the rotational degrees of freedom of the side chains may be a significant contributor to the overall entropy of the protein conformation (17). Lattice protein models also lose details of the different interactions between protein residues, such as Coulomb interactions, salt bridges, disulphide bonds, etc. Although the relative influence of these factors on protein stability is still poorly understood (18,19), lattice protein models capture the basic physics of the hydrophobic-effect-dominated protein folding (16,20–24). The simplicity of these models allows us to perform detailed calculations of the free energy landscape, which is not possible for the more complex models.

We studied a 64-mer four-helix bundle and a 42-mer protein, designed by Yue and Dill (20). Both these protein sequences undergo a thermal folding transition like real proteins (21). In addition to an isolated protein, we studied the adsorption of a two-protein system to understand the role of interprotein interactions. Whereas a proper study would involve a finite number (hopefully large) of proteins near surfaces, detailed simulations of 10 64-mer lattice protein molecules showed that the simulations can get kinetically trapped in different metastable states. Therefore, we were never sure if the simulations realized the equilibrium states of these systems. (It is hard to perform a proper free-energy analysis, or alternatively a density of states calculation, for such a large number of molecules.) The two-protein case is not hindered by these constraints, and is thus a good compromise model for understanding the role of interprotein interactions.

In the simulation box, the hydrophobic surface is placed at $z = 0$ and an athermal surface is placed at $z = z_{\max}$ with periodic boundary conditions in lateral directions. The value $z_{\max}$ is taken equal to the protein chain length, which is much larger than the mean-squared radius of gyration of the protein at the simulated temperatures. The simulation box size is 64×64 lattice units in the x and y directions for the single-protein case and 16×16 lattice units for the two-protein case. The smaller lateral dimensions were chosen to study the effect of concentration, but still they were larger than the largest average radius of gyration (~4.5) at the studied temperatures, implying only minimal interaction between the protein and its periodic image. To ensure that there are no confinement effects, we compared the simulations of proteins in the bulk (that is, no surface) with those done at $\lambda_s = 0$. Both the simulations gave same results (same melting temperature, specific heat curve, etc.). We conjecture that, because the proteins do not adsorb to the surface for $\lambda_s = 0$, and because the periodic box size is much bigger than the radius of gyration of the chains, the surface plays no role in this limit.

The energy of the multiprotein system is given by

$$E = \sum_{m=1}^{k}\sum_{i_m=1}^{n_m-2}\sum_{j_m=i_m+2}^{n_m}\varepsilon_{i_m j_m}\left(r_{i_m j_m}\right) + \sum_{m=1}^{k}\sum_{i_m=1}^{n_m}\lambda_s\varepsilon_{i_m s}\left(r_{i_m s}\right) + \sum_{m=1}^{k-1}\sum_{p=m+1}^{k}\sum_{i_m=1}^{n_m}\sum_{j_p=1}^{n_p}\lambda_{\mathrm{mut}}\varepsilon_{i_m j_p}\left(r_{i_m j_p}\right). \quad (1)$$

Equation 1 is the sum of the internal energy, the protein-surface interaction energy, and the interprotein interaction energy. The expression $\varepsilon_{ij}(r_{ij})$ represents the interaction energy between beads i and j, where i and j can be either H or P. The value λ_{mut} is a restraining potential to ensure efficient sampling of the conformational space for a better estimate of the density of states (DOS). Once a good sampling of the conformational space is achieved, the bias introduced by λ_{mut} is removed by using the weighted histogram analysis method (25–27).

Multiple canonical ensemble Monte Carlo (MC) (28) simulations at different $T^*(= k_B T/|\varepsilon_{H\text{-}H}(1)|)$ and λ_s, for the single protein molecule, and at different temperatures T^*, λ_s, and λ_{mut} for the two protein molecules, were performed. The attempted MC moves consisted of local moves such as end-bond flip, internal bond flip, and crankshaft moves (29) as well as configurationally biased Monte Carlo moves (30). The simulation data was combined by using the weighted histogram analysis method to get the DOS. For the single protein case, ~420 different MC simulations were performed to get the DOS as a two-dimensional function of intraprotein and protein-surface interactions. For the two-protein case, ~4600 different MC simulations were performed to get the DOS as a three-dimensional function of intraprotein, interprotein, and protein-surface interactions.

Transition path sampling (31) was attempted, but huge and multiple kinetic barriers were observed. Because of this, we were unable to generate transition paths between the folded and the unfolded conformations at relevant temperatures. An important point here is that there is no unique descriptor(s) for describing the order parameters relevant to the unfolding or folding of these model proteins. We thus use two descriptors (the number of intrachain hydrophobic contacts, also termed as the internal energy states, E_{intra} and the fraction of native hydrophobic intrachain contacts, N_{native}) to describe intraprotein interactions to ensure ourselves that the results obtained for the relevant activated state derived by our analysis is not an artifact of our (arbitrarily) chosen order parameter variable. Because the free energy landscape of the two-protein case is a three-dimensional function of intraprotein, interprotein, and protein-surface interactions, there can be multiple pathways between different points on the free energy landscape. Therefore, to estimate the unfolding free energy barrier on this free energy landscape, we assumed that in one kinetic step, a protein molecule can only hop from one energy state to another, which is not very different from the initial energy state with respect to the number and kind of interactions. The probability of a hop from one energy state to the other is proportional to the ratio of Boltzmann weights of the two energy states. That is, the probability to go from a state A to a state B is proportional to

$$e^{-\Delta G_{AB}/k_B T},$$

where $\Delta G_{AB} = G_B\text{-}G_A$. G_x is the free energy of the state x. Using this approach, many (~200) MC walks in the free-energy landscape, from the folded-adsorbed ensemble to the most stable unfolded ensemble, were generated. The unfolding free energy barrier for each walk was taken as the difference between the largest value of the free energy encountered in

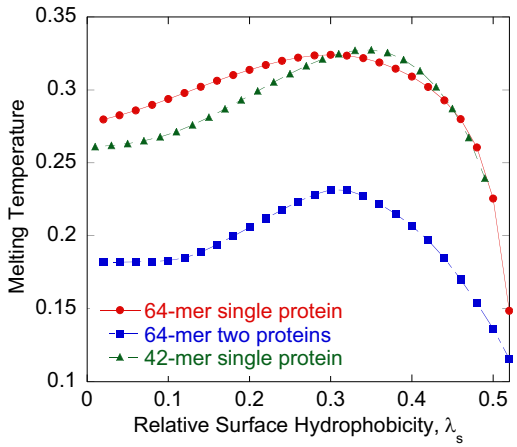

FIGURE 1 A plot of melting temperature of the isolated 64-mer protein, the isolated 42-mer protein, and the two 64-mer protein molecules as a function of λ_s.

the walk with that of the folded-adsorbed state. An MC walk in the free energy landscape is computationally faster than a walk in the conformational space. Here, we have assumed that energetically close states are structurally close also, and hence kinetically accessible to each other, but this may not be true. Conformations, when identified by only three order parameters, can be structurally quite different from one other.

RESULTS

Single protein

A single 64-mer protein in bulk solution has a melting temperature, T_m of $T^* = 0.28$ (21) in reduced units (see Methods). T_m is the temperature when the free energy of the folded protein is equal to that of the unfolded protein. Fig. 1 shows that the T_m of the 64-mer single protein first increases monotonically with λ_s, reaches a maximum in the vicinity of $\lambda_s \sim 0.3$–0.4, and then monotonically decreases. For $\lambda_s > 0.45$, the T_m of the protein becomes smaller than that in the bulk, and therefore, the surface becomes a destabilizing one. Also shown in Fig. 1 is the T_m of a 42-mer single protein (20) as function of λ_s, which shows the same trend as the 64-mer. To prove that the proteins are indeed adsorbed in the region of interest ($\lambda_s \sim 0.2$–0.5), we have shown in Fig. S2 in the Supporting Material that the adsorption transition temperature is higher than the bulk melting temperature.

Comparison with experiments suggests that:

1. We have a good agreement with the apparently universal conclusion that chains in dilute concentration on hydrophobic surfaces are stabilized relative to the solution state.
2. The experimental systems correspond to relatively modest λ_s values.

Below, we explore the origins of 1 above.

To understand why the folded state is stabilized for low-to-intermediate values of λ_s, we construct the thermodynamic cycle

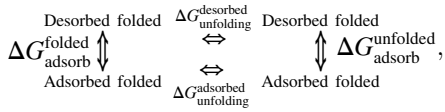

which incorporates the four states of interest—namely the folded and unfolded states in both the bulk solution and at the surface. Because the net free energy change traversing the cycle must exactly equal zero, we obtain the identity

$$\Delta G^{\text{desorbed}}_{\text{unfolding}} + \Delta G^{\text{unfolded}}_{\text{adsorb}} = \Delta G^{\text{adsorbed}}_{\text{unfolding}} + \Delta G^{\text{folded}}_{\text{adsorb}}.$$

Let us now consider a temperature corresponding to the T_m of the desorbed protein, $\Delta G^{\text{desorbed}}_{\text{unfolding}} = 0$. For us to obtain the experimental result that the folded state is stabilized on adsorption, it then follows that at this temperature, $\Delta G^{\text{adsorbed}}_{\text{unfolding}} > 0$. This immediately yields that $\Delta G^{\text{unfolded}}_{\text{adsorb}} - \Delta G^{\text{folded}}_{\text{adsorb}} > 0$, namely that the free energy of adsorbing the folded state is more favorable than that for the unfolded state.

Two questions now naturally arise:

Do the simulations verify this experimentally inspired conclusion?

What are the molecular origins of this effect?

Fig. 2 *a* shows a plot of the free energy of adsorption of the folded state, $\Delta G^{\text{folded}}_{\text{adsorb}}$ and the unfolded state, $\Delta G^{\text{unfolded}}_{\text{adsorb}}$, as a function of λ_s at $T^* = T_m = 0.28$. The $\Delta G^{\text{folded}}_{\text{adsorb}}$ is favorable because the favorable interactions of the exposed H-groups in the folded state of the protein with the surface overcome the loss in translational entropy upon adsorption. Haynes and Norde (17) calculated that the hydrophobic groups occupy 40–60% of the water-accessible surface area in Lysozyme. Meirovitch and Scheraga (32) put the corresponding number at ~13%. For both the 64-mer and the 42-mer protein molecules, there are six hydrophobic beads that interact with the surface in the folded-adsorbed state. From Fig. 2 *a*, it is clear that for low-to-intermediate λ_s, the $\Delta G^{\text{folded}}_{\text{adsorb}}$ is more favorable than $\Delta G^{\text{unfolded}}_{\text{adsorb}}$. Under these conditions, the protein conformations on a hydrophobic surface are stabilized. For larger λ_s, this trend reverses and the folded state is destabilized.

To isolate the importance of energetic and entropic effects, in Fig. 2 *b*, we plot $\Delta E^{\text{folded}}_{\text{adsorb}} - \Delta E^{\text{unfolded}}_{\text{adsorb}}$ and $T\Delta S^{\text{folded}}_{\text{adsorb}} - T\Delta S^{\text{unfolded}}_{\text{adsorb}}$ for the single protein as a function of λ_s. Over the entire range of λ_s, change in energy upon adsorbing the unfolded protein, $\Delta E^{\text{unfolded}}_{\text{adsorb}}$ is more favorable than that of the folded protein, $\Delta E^{\text{folded}}_{\text{adsorb}}$. Therefore, energetically, it is always preferred to adsorb an unfolded protein. However, for $\lambda_s < 0.45$, the loss in entropy upon adsorption of the unfolded protein, $T\Delta S^{\text{unfolded}}_{\text{adsorb}}$ is much larger than that of the folded protein, $T\Delta S^{\text{folded}}_{\text{adsorb}}$. Also, for $\lambda_s < 0.45$, $T\Delta S^{\text{folded}}_{\text{adsorb}} - T\Delta S^{\text{unfolded}}_{\text{adsorb}} > \Delta E^{\text{folded}}_{\text{adsorb}} - \Delta E^{\text{unfolded}}_{\text{adsorb}}$. Thus, entropic effects dominate the energetic ones, and the protein molecule prefers to adsorb on the hydrophobic surface in the folded state. The loss in entropy upon adsorption has

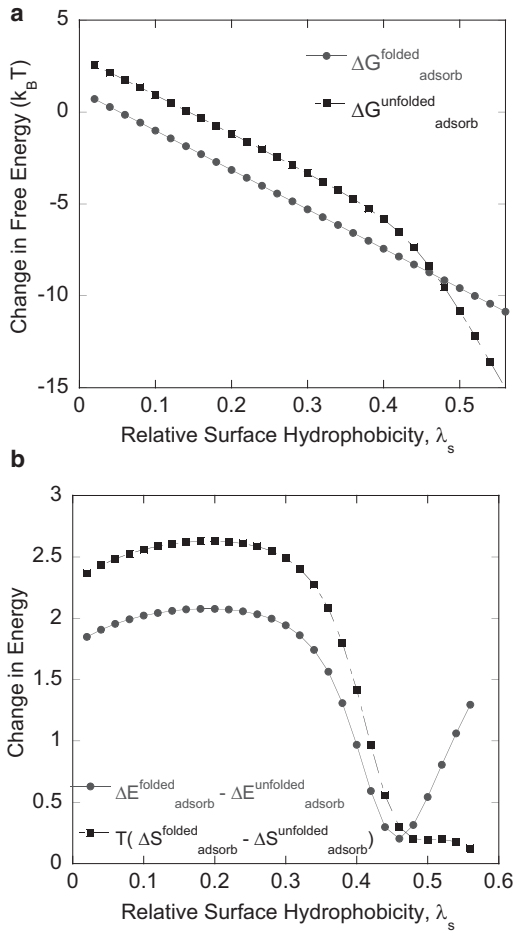

FIGURE 2 A plot of (*a*) the free energy of adsorbing the single 64-mer protein in the folded state, $\Delta G^{folded}_{adsorb}$ and in the unfolded state, $\Delta G^{unfolded}_{adsorb}$; and (*b*) the difference between the energy of adsorbing the folded and the unfolded single 64-mer protein, $\Delta E^{folded}_{adsorb} - \Delta E^{unfolded}_{adsorb}$ and the difference between the entropy of adsorbing the folded protein and the unfolded single 64-mer protein $T\Delta S^{folded}_{adsorb} - T\Delta S^{unfolded}_{adsorb}$ as a function of λ_s at $T^* = T_m = 0.28$.

been predicted before for two-dimensional protein models (33,34). Beyond $\lambda_s \sim 0.45$, the adsorption of the unfolded protein molecule is preferred because the energetic gain of adsorbing the unfolded protein molecule dominates over the loss in entropy accompanying it. Therefore, the stability of the folded state of the protein on hydrophobic surfaces can be attributed to the large entropic loss associated with adsorbing an unfolded protein molecule. However, highly hydrophobic surfaces denature proteins upon adsorption because the hydrophobic core of the protein tends to open up and adsorb strongly on such a surface. Fig. S6 and the accompanying discussion in the Supporting Material explains the behavior of the absolute values of the change in energy and entropy associated with adsorbing a folded and an unfolded protein from the bulk to the surface as a function of λ_s. ΔE_{folded} is a linearly decreasing function of λ_s. This is because the protein in its folded state makes six hydrophobic contacts with the surface and so, $\Delta E_{folded} = -6\ \lambda_s$. $\Delta E_{unfolded}$ is always more negative than ΔE_{folded}. $T\Delta S_{folded}$ does not depend on λ_s, because it is just the loss in translational entropy of the folded protein upon adsorption. $T\Delta S_{unfolded}$ is much more negative than the $T\Delta S_{folded}$ for $\lambda_s < 0.45$. This shows that adsorption of an unfolded protein is entropically much less favored than that of the folded protein for $\lambda_s < 0.45$.

Two proteins

Fig. 1 shows that for the two protein molecules, the T_m in the bulk is 0.18, which is significantly lower than that of the single protein molecule. This implies that the protein becomes less stable with an increase in concentration. When a protein molecule unfolds, it loses internal energy but gains conformational entropy. At T_m, the loss in internal energy is exactly balanced by the gain in conformational entropy. However, in the presence of a second protein molecule, the unfolded conformations are also stabilized by interprotein interactions. This leads to a net decrease in the T_m. This conclusion is consistent with the previous findings of Gupta et al. (35), who had deduced that aggregation competes with protein folding with increased concentration. However, these previous workers only performed canonical ensemble simulations and hence could not decide which of these states represent equilibrium. Similar to the single protein case, the two protein molecules are also stabilized upon adsorption on small-to-intermediately hydrophobic surfaces (see Fig. 1) because of the reasons discussed above. Thus, at each concentration, adsorption stabilizes the folded state, while the unfolded state only dominates for strongly adsorbing surfaces.

Folding/unfolding barriers

Our simulation results show that protein stability is highly dependent on solution concentration. According to Fig. 1, three scenarios exist:

First scenario. The experimental temperature, T_{exp}, is less than the melting temperature of both the concentrated protein solution, T_{conc} and that of the dilute protein solution, T_{dil}. In such a case, the proteins will be folded in both the bulk and the adsorbed states.

Second scenario. When $T_{exp} > T_{dil} > T_{conc}$, the proteins will be unfolded in both the bulk and the adsorbed states.

Third scenario. This case, in which $T_{dil} > T_{exp} > T_{conc}$, is particularly interesting, and is the one that we think is relevant to most experiments.

In the case of the third scenario, it would mean that in concentrated solutions, such as, in a cellular environment, the global minimum of the free energy may be the unfolded-aggregated state. However, it is empirically well recognized that proteins do not readily denature under

such conditions. Because the thermodynamics of this situation favor the unfolded-aggregated state, probably the kinetic factors override them and prevent the unfolding process from occurring. To understand the kinetics of unfolding, we estimated the unfolding free energy barriers of the single and the two-protein system. One way to estimate the free energy barriers is to do a transition path sampling (31) between the two conformational ensembles of interest. However, our attempts to generate transition paths between the folded and the unfolded ensemble failed because of huge and multiple kinetic barriers at temperatures of interest ($T^* < T_m$). Therefore, to estimate the unfolding free energy barriers, we did a stochastic walk in the multidimensional free energy landscape.

For the single-protein case, the free energy landscape was generated as a function of two sets of order parameters: (N_{native}, N_s) and (E_{intra}, N_s), where N_{native} is the fraction of native contacts in a conformation, N_s is the number of H groups of the protein in contact with the surface, and E_{intra} is the internal energy of the protein molecule. For the two-protein case, the free energy landscape was generated as a three-dimensional function of (N_{native}, N_s, E_{inter}) and (E_{intra}, N_s, E_{inter}), where E_{inter} is the interprotein interaction energy. The method of estimating the unfolding free energy barriers has been described in Materials and Methods in more detail. Fig. 3 shows the unfolding free energy barriers at $T^* = 0.2$. For the single-protein case, for $\lambda_s < 0.3$, the free energy landscape is approximately a smooth funnel (see Fig. S1 *a*) and hence unfolding free energy barriers were not estimated for this range. The unfolding free energy barrier is ~22 k_BT at $\lambda_s = 0.32$, and decreases monotonically as the λ_s increases. For the two-protein case, an ensemble of unfolded states is always a local minimum in the free energy landscape irrespective of the value of λ_s (see Fig. S1 *b*).

For the two-protein case, for $\lambda_s < 0.3$, the unfolding free energy barriers are independent of the λ_s value. For the (N_{native}, N_s, E_{inter}) set of order parameters, the unfolding free energy barriers for $\lambda_s < 0.3$ are ~29 k_BT, whereas for (E_{intra}, N_s, E_{inter}), they are ~26 k_BT. For $\lambda_s > 0.3$, the unfolding free energy barriers decrease as the λ_s increases. The observed decrease in the unfolding free energy barrier is reasonable because as the surface becomes more hydrophobic, it can stabilize the transition states better, which have more exposed hydrophobic groups. In this respect, the hydrophobic surface acts like a heterogeneous catalyst. It stabilizes the transition state, thereby increasing the rate of unfolding. The unfolding free energy barriers determined using (N_{native}, N_s, E_{inter}) follow the trends determined using (E_{intra}, N_s, E_{inter}) with a small offset (3 k_BT). This offset is not surprising when the relationship between N_{native} and E_{intra} is analyzed carefully (see Fig. S7). The unfolding free energy barriers for the two-protein case are larger than for the single-protein case because the two protein molecules can associate in the folded state and further stabilize themselves.

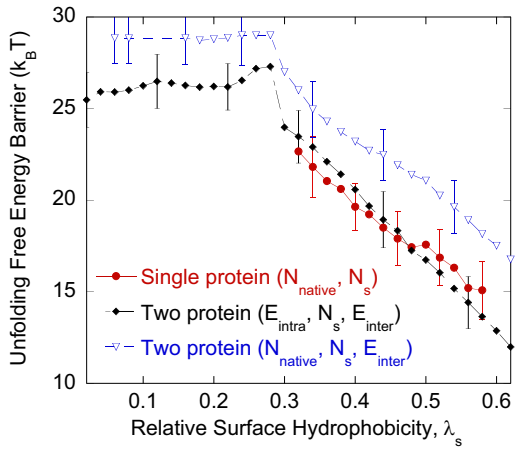

FIGURE 3 An estimate of unfolding free energy barriers as a function of λ_s at $T^* = 0.2$ for the single and two 64-mer protein molecules determined by multiple Monte Carlo walks from the folded-adsorbed ensemble to the most stable unfolded ensemble in the multidimensional free energy landscape. For the single-protein case, the free energy landscape is a function of (N_{native}, N_s) and for the two-protein case, the free energy landscape is a three-dimensional function of (N_{native}, N_s, E_{inter}) and (E_{intra}, N_s, E_{inter}). Error bars are the standard deviation in the estimate of the free energy barriers from 200 MC paths.

An important conclusion is that although increasing protein concentration shows a decrease in the stability of proteins in the bulk, because of the large unfolding free energy barriers, the unfolding and aggregation of the protein molecules are kinetically hindered. However, presence of a hydrophobic surface decreases the unfolding free energy barrier. This explains the experimental results of proteins adsorbing at large concentrations. Proteins, in the folded state in the bulk, denature upon adsorption for two reasons:

First, near the surface, there is an increased local concentration of the protein molecules, and hence the folded state becomes less stable.

Second, the presence of the hydrophobic surface brings down the unfolding free energy barrier, thereby promoting protein denaturation and aggregation.

Inasmuch as this is an equilibrium study, we do not directly get any information about the pathway of protein adsorption. However, from the results of the unfolding free energy barriers, we can comment on the probable pathway for the observed conformational changes that occur. Fig. 3 shows that there are large unfolding free energy barriers in the bulk. The magnitude of the barriers decreases in the adsorbed state. Therefore, we speculate that the protein molecules would first adsorb onto the surface in the folded state and then unfold on the surface. This statement is given credibility by the fact that the proteins do not unfold and aggregate in the solution. The surface therefore acts as a catalyst to unfolding. The kinetics of protein unfolding is likely to be influenced by the presence of water molecules, whereas our analysis accounts for the effect of water only implicitly. Therefore, a study involving explicit

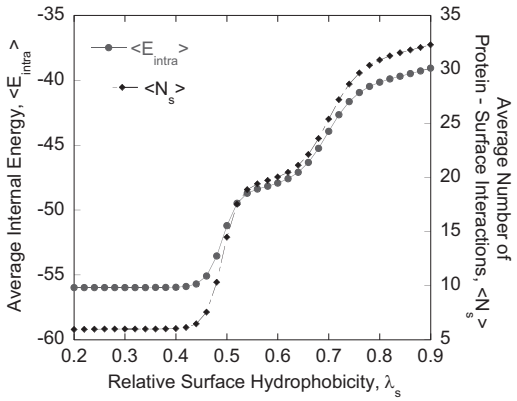

FIGURE 4 A plot of the average internal energy, $\langle E_{\text{intra}} \rangle$ and the average number of protein-surface interactions, $\langle N_s \rangle$ of a 64-mer protein molecule as a function of λ_s at $T^* = 0.2$.

water molecules may show different magnitude of free-energy barriers. However, a surface-stabilized transition state looks intuitively probable in such a case also, and hence a similar trend in the variation of free energy barriers with respect to surface hydrophobicity is speculated.

Regimes of adsorbed proteins

In the above set of results, we only focused on the stability of the folded state of the proteins. In this section, we probe the conformational states of the proteins near surfaces of varying hydrophobicities. Fig. 4 shows the average internal energy, $\langle E_{\text{intra}} \rangle$ and the average number of protein-surface interactions, $\langle N_s \rangle$ for the single protein as a function of λ_s at $T^* = 0.2$. The protein remains in the folded-adsorbed state for $0.08 < \lambda_s < 0.45$, beyond which it exists in the unfolded-adsorbed state. In the unfolded-adsorbed state, the single protein molecule undergoes a weak-to-strong

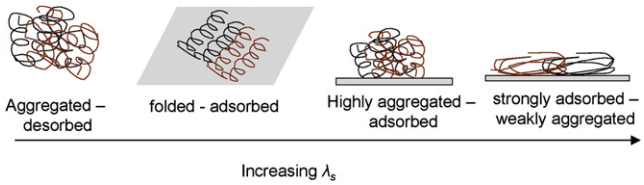

FIGURE 6 A cartoon showing different regimes of the two 64-mer protein molecules near a hydrophobic surface as a function of λ_s at $T^* = 0.2$.

adsorption transition at $\lambda_s \sim 0.66$, as indicated by a jump in the $\langle N_s \rangle$.

The free energy of adsorbing a folded state, $\Delta G^{\text{folded}}_{\text{adsorb}}$ and the unfolded state, $\Delta G^{\text{unfolded}}_{\text{adsorb}}$ for the two-protein case is plotted in Fig. 5 as a function of λ_s at $T^* = 0.2$. At $T^* = 0.2$, the proteins are aggregated in the bulk as the T_m for the two-protein case is 0.18. $\Delta G^{\text{folded}}_{\text{adsorb}} \sim 0 < \Delta G^{\text{unfolded}}_{\text{adsorb}}$ at λ_s ~0.12, and $\Delta G^{\text{unfolded}}_{\text{adsorb}} < \Delta G^{\text{folded}}_{\text{adsorb}} < 0$ for $\lambda_s > 0.42$. This implies that the proteins exist in the aggregated-desorbed state in the bulk for weakly hydrophobic surfaces ($\lambda_s < 0.14$), and folded-adsorbed state for intermediately hydrophobic surfaces ($0.14 < \lambda_s < 0.42$). Beyond $\lambda_s \sim 0.42$, the proteins adsorb in the unfolded state. The difference in the free energy between the adsorbed and the desorbed states, $\Delta G_{\text{ads-des}}$, is a monotonically decreasing function of λ_s. To examine the conformational states of the unfolded-adsorbed proteins, we studied the behavior of different thermodynamic properties as a function of λ_s. In the unfolded-adsorbed state, the proteins can exist in highly aggregated-adsorbed and weakly aggregated-strongly adsorbed regimes. Fig. 6 pictorially shows different regimes of the proteins as a function of λ_s at $T^* = 0.2$. The existence of these regimes is shown with the help of Fig. 7, in which the average internal energy of the proteins, $\langle E_{\text{intra}} \rangle$ and the average interprotein interaction energy, $\langle E_{\text{inter}} \rangle$ have been plotted as a function of λ_s. Other thermodynamic properties

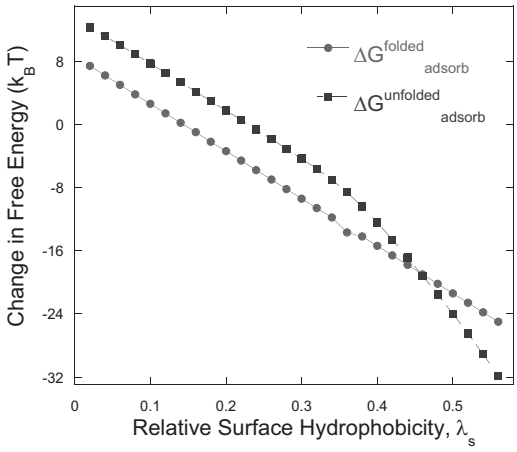

FIGURE 5 A plot of the free energy of adsorbing the two 64-mer protein molecules in the folded, $\Delta G^{\text{folded}}_{\text{adsorb}}$ and the unfolded state, $\Delta G^{\text{unfolded}}_{\text{adsorb}}$ as a function of λ_s at $T^* = 0.2$.

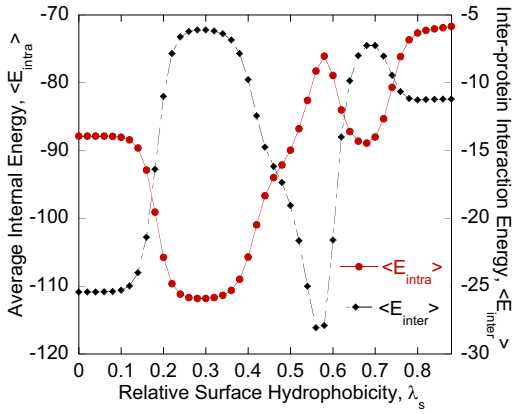

FIGURE 7 A plot of the average internal energy, $\langle E_{\text{intra}} \rangle$ and the average interprotein interaction energy, $\langle E_{\text{inter}} \rangle$ of the two 64-mer protein molecules as a function of λ_s at $T^* = 0.2$.

such as the average number of H-surface contacts, $\langle N_s \rangle$, and the conformational entropy, S, as a function of λ_s, have been shown in Fig. S3. Fig. S4 shows typical conformations of the two protein molecules in different regimes. Below we discuss the observations from Fig. 7 in detail.

Aggregated-desorbed regime

For $\lambda_s < 0.12$, the proteins exist in the aggregated-desorbed state. In this state, there is a significant degree of interprotein association ($\langle E_{\text{inter}} \rangle \sim -27$).

Folded-adsorbed regime

At λ_s ~0.14, there is a clear transition from the unfolded-aggregated state to the folded ($\langle E_{\text{intra}} \rangle \sim -112$), adsorbed ($\langle N_s \rangle$ ~12), and dimeric ($\langle E_{\text{inter}} \rangle \sim -6$) state ($T_m$ of the proteins goes above 0.2 (Fig. 1)). Folding of the protein molecules is accompanied by a sharp drop in S. The decrease in $\Delta G_{\text{ads-des}}$ is therefore energetically driven, which overrides the unfavorable decrease in S.

Strongly aggregated-adsorbed regime

For $\lambda_s > 0.42$, the T_m falls below 0.2 (Fig. 1), and the proteins unfold in the adsorbed state. For λ_s ~0.42 to 0.58, $\langle E_{\text{intra}} \rangle$ increases because of protein unfolding. A sharp drop in $\langle E_{\text{inter}} \rangle$ is observed, implying that the two protein molecules are now strongly aggregated. Therefore, as λ_s goes from 0.42 to 0.58, there is a continuous transition from the folded-adsorbed regime to the highly aggregated-adsorbed regime, with a loss in intraprotein interaction in lieu of interprotein interactions. A large gain in S is observed, which overcomes the unfavorable increase in the total energy of the system.

Weakly aggregated-adsorbed regime

At $\lambda_s \sim 0.58$, there is clearly another transition in the adsorbed state of the proteins. There is an increase in $\langle N_s \rangle$ to ~60, which means that the protein molecules are now strongly adsorbed on the surface. This occurs at the expense of interprotein interactions, which is reflected in an increase in $\langle E_{\text{inter}} \rangle$. Therefore, at these values of λ_s, the proteins are in a strongly adsorbed and weakly aggregated state. A decrease in $\langle E_{\text{intra}} \rangle$ is observed, implying that the protein forms an added number of intraprotein contacts. There is a decrease in S as a consequence of strong adsorption.

DISCUSSION

Relationship to previous works

First, we ask if the entopic stabilization of the folded state on weakly adsorbing surfaces might be understood in the context of existing theories. In particular, we point to the pioneering work of Zhou and Dill (36), who suggested that the confinement of proteins in "cages" served to stabilize the folded state. This profound conclusion follows from the fact that on confinement there is a loss of entropy of unfolded proteins, while the folded conformation is essentially unaffected. Experimental evidence does support their idea (37,38). At first sight it would appear that adsorption of proteins is a situation where the enthalpy of adsorption has to overcome large entropy effects. However, this argument is only partially correct. In the weak adsorption limit, a protein needs to only gain a k_BT in interaction strength to overcome its translational entropy to adsorb. Thus, a chain can adsorb without substantial changes to its bulk conformation, suggesting that the purely conformational entropy ideas of Zhou and Dill apply well in the context of the adsorption of proteins. Our newer results on the effects of protein concentration on the thermodynamics and kinetics of unfolding, however, do not seem to be considered in previous works.

Do experiments support the theoretical results?

Our theoretical calculations suggest that at low concentrations, hydrophobic surfaces stabilize the folded conformation, while the chains unfold at higher concentrations and then refold into β-sheets or remain as random coils. (Regardless, at higher concentration there is a decrease in α-helix content on adsorption.) Table 1, which corresponds to experimental results where there is essentially no change in structure, are indeed in the regime where the amount adsorbed is low, with fractional surface coverages typically <0.4. (The only exception to this rule is cutinase; at the time of this writing, we do not understand why this molecule behaves differently.) In contrast, Table 2, which contains experimental data for Lysozyme on a variety of surfaces (15), indeed shows a progressive decrease in α-helix content for fractional coverage >0.6. Upon adsorption on Teflon at low fractional coverages (<0.1) hydrophobin SC3 attains an α-helical conformation, whereas it attains an intermolecular β-sheet rich conformation when interprotein interactions are promoted (10,11). Experimental evidence also suggests that a decrease in interprotein

TABLE 2 Changes in lysozyme structure on surfaces of different polarities (15)

Surface material	Adsorbed amount (mg/m^2)	Fractional surface coverage	Water contact angle (degrees)	% loss of helix
RC	1.2	0.6	27	5
PVP-PES	1.8	0.8	48	20
PES	2	0.9	55	30
PTFE	2.5	1.1	120	45

Fractional surface coverages were calculated by assuming adsorbed proteins' dimensions equal to that of the native state with "flat-on" orientation.

interactions between adsorbed proteins achieved either by adsorbing them on curved nanoscale surfaces (39) or on patchy surfaces with adsorbing and nonadsorbing regions (40) indeed increase the stability of the adsorbed proteins. These data unequivocally support our primary conclusions for the importance of surface coverage in determining the stability of proteins adsorbed on hydrophobic surfaces.

Generality of theoretical results

The foldable 42-mer, single-protein molecule (20) also showed an increase in thermal stability upon adsorption on intermediately hydrophobic surfaces (Fig. 1). Simulations of adsorption of two 42-mer lattice protein molecules on a hydrophobic surface show similar regimes to that of the 64-mer protein (see Fig. S5). This proves the generality of our results.

Is there an optimal order parameter?

It is important to realize that no matter what order parameter is used, they always average out the extremely large dimensional conformational space to a lower dimensional space, which leads to loss of some information. Which order parameter best represents a particular system is still an open question. A comparison of the two order parameters used by us—the fraction of native contacts, N_{native} and the total internal energy, E_{intra}—shows that N_{native} is a better order parameter than E_{intra} (see Fig. S7).

CONCLUSIONS

Intermediately hydrophobic surfaces can thermally stabilize the folded state of the adsorbed protein. This happens because the unfolded state of the protein experiences significant loss of entropy upon adsorption, and hence the protein prefers to remain in the folded state. The gain in secondary structure in proteins upon adsorption may also be due to preference of the protein chain to remain folded near the hydrophobic surface. Highly hydrophobic surfaces, however, perturb the secondary structure of the proteins. Interprotein interactions can significantly reduce stability of the proteins, although large unfolding free energy barriers in the bulk probably prevent spontaneous protein aggregation. Hydrophobic surfaces lower the unfolding free energy barriers. This explains why proteins can denature on adsorption at large concentrations. Depending on the value of surface hydrophobicity, the proteins can exist in different regimes—namely, the aggregated-desorbed, folded-adsorbed, highly aggregated-adsorbed, and weakly aggregated-strongly adsorbed regimes. All of these results appear to be in good qualitative agreement with experiments, suggesting that we have a good understanding of a broad range of experimental data, which has remained little understood to this time.

SUPPORTING MATERIAL

Seven figures and five equations are available at http://www.biophysj.org/biophysj/supplemental/S0006-3495(10)00668-5.

We thank Dr. Georges Belfort and Gaurav Anand (Rensselaer Polytechnic Institute, Troy, NY), our long-term collaborators on this project.

S.S. and S.K.K. thank the Department of Energy (Basic Energy Sciences) for funding this research. B.J.B. acknowledges support of this project from the National Institutes of Health under grant No. GM-4330.

REFERENCES

1. Wallqvist, A., and B. J. Berne. 1995. Computer simulation of hydrophobic hydration forces on stacked plates at short range. *J. Phys. Chem.* 99:2893–2899.
2. Lum, K., D. Chandler, and J. D. Weeks. 1999. Hydrophobicity at small and large length scales. *J. Phys. Chem. B.* 103:4570–4577.
3. Jamadagni, S. N., R. Godawat, …, S. Garde. 2009. How interfaces affect hydrophobically driven polymer folding. *J. Phys. Chem. B.* 113:4093–4101.
4. Vermeer, A. W. P., C. E. Giacomelli, and W. Norde. 2001. Adsorption of IgG onto hydrophobic Teflon. Differences between the F(ab) and F (c) domains. *Biochim. Biophys. Acta.* 1526:61–69.
5. Norde, W., and C. E. Giacomelli. 1999. Conformational changes in proteins at interfaces: from solution to the interface, and back. *Macromol. Symp.* 145:125–136.
6. Zoungrana, T., G. H. Findenegg, and W. Norde. 1997. Structure, stability, and activity of adsorbed enzymes. *J. Colloid Interface Sci.* 190:437–448.
7. Mollmann, S. H., L. Jorgensen, …, S. Frokjaer. 2006. Interfacial adsorption of insulin conformational changes and reversibility of adsorption. *Eur. J. Pharm. Sci.* 27:194–204.
8. Giacomelli, C. E., and W. Norde. 2003. Influence of hydrophobic Teflon particles on the structure of amyloid β-peptide. *Biomacromolecules.* 4:1719–1726.
9. Giacomelli, C. E., and W. Norde. 2005. Conformational changes of the amyloid β-peptide (1–40) adsorbed on solid surfaces. *Macromol. Biosci.* 5:401–407.
10. Wang, X., M. L. de Vocht, …, G. T. Robillard. 2002. Structural changes and molecular interactions of hydrophobin SC3 in solution and on a hydrophobic surface. *Protein Sci.* 11:1172–1181.
11. de Vocht, M. L., K. Scholtmeijer, …, G. T. Robillard. 1998. Structural characterization of the hydrophobin SC3, as a monomer and after self-assembly at hydrophobic/hydrophilic interfaces. *Biophys. J.* 74: 2059–2068.
12. Maste, M. C. L., W. Norde, and A. J. W. G. Visser. 1997. Adsorption-induced conformational changes in the serine proteinase savinase: a tryptophan fluorescence and circular dichroism study. *J. Colloid Interface Sci.* 196:224–230.
13. Maruyama, T., S. Katoh, …, K. Satoh. 2001. FT-IR analysis of BSA fouled on ultrafiltration and microfiltration membranes. *J. Membr. Sci.* 192:201–207.
14. Sethuraman, A., and G. Belfort. 2005. Protein structural perturbation and aggregation on homogeneous surfaces. *Biophys. J.* 88:1322–1333.
15. Sethuraman, A., G. Vedantham, …, G. Belfort. 2004. Protein unfolding at interfaces: slow dynamics of α-helix to β-sheet transition. *Proteins: Struct. Funct. Bioinf.* 56:669–678.
16. Dill, K. A. 1990. Dominant forces in protein folding. *Biochemistry.* 29:7133–7155.
17. Haynes, C. A., and W. Norde. 1995. Structures and stabilities of adsorbed proteins. *J. Colloid Interface Sci.* 169:313–328.
18. Kajander, T., P. C. Kahn, …, A. Goldman. 2000. Buried charged surface in proteins. *Structure.* 8:1203–1214.

19. Honig, B., and A. S. Yang. 1995. Free energy balance in protein folding. *Adv. Protein Chem.* 46:27–58.

20. Yue, K., and K. A. Dill. 1995. Forces of tertiary structural organization in globular proteins. *Proc. Natl. Acad. Sci. USA.* 92:146–150.

21. Sharma, S., and S. K. Kumar. 2008. Finite size effects on locating conformational transitions for macromolecules. *J. Chem. Phys.* 129:134901.

22. Lattman, E. E., K. M. Fiebig, and K. A. Dill. 1994. Modeling compact denatured states of proteins. *Biochemistry.* 33:6158–6166.

23. Cellmer, T., D. Bratko, …, H. Blanch. 2005. Protein-folding landscapes in multichain systems. *Proc. Natl. Acad. Sci. USA.* 102:11692–11697.

24. Castells, V., S. X. Yang, and P. R. Van Tassel. 2002. Surface-induced conformational changes in lattice model proteins by Monte Carlo simulation. *Phys. Rev. E Stat. Nonlin. Soft Matter Phys.* 65:031912.

25. Kumar, S., D. Bouzida, …, J. M. Rosenberg. 1992. The weighted histogram analysis method for free-energy calculations on biomolecules. 1. The method. *J. Comput. Chem.* 13:1011–1021.

26. Ferrenberg, A. M., and R. H. Swendsen. 1989. Optimized Monte Carlo data analysis. *Phys. Rev. Lett.* 63:1195–1198.

27. Chodera, J. D., W. C. Swope, …, K. A. Dill. 2007. Use of the weighted histogram analysis method for the analysis of simulated and parallel tempering simulations. *J. Chem. Theory Comput.* 3:26–41.

28. Allen, M. P., and D. J. Tildesley. 1987. Computer Simulation of Liquids. Oxford University Press, New York.

29. Hilhorst, H. J., and J. M. Deutch. 1975. Analysis of Monte-Carlo results on kinetics of lattice polymer-chains with excluded volume. *J. Chem. Phys.* 63:5153–5161.

30. Siepmann, J. I., and D. Frenkel. 1992. Configurational bias Monte-Carlo—a new sampling scheme for flexible chains. *Mol. Phys.* 75:59–70.

31. Bolhuis, P. G., C. Dellago, …, D. Chandler. 2000. Transition path sampling: throwing ropes over mountains in the dark. *J. Phys. Condens. Matter.* 12:A147–A152.

32. Meirovitch, H., and H. A. Scheraga. 1980. Empirical-studies of hydrophobicity. 2. Distribution of the hydrophobic, hydrophilic, neutral, and ambivalent amino-acids in the interior and exterior layers of native proteins. *Macromolecules.* 13:1406–1414.

33. Wattenbarger, M. R., H. S. Chan, …, K. A. Dill. 1990. Surface-induced enhancement of internal structure in polymers and proteins. *J. Chem. Phys.* 93:8343–8351.

34. Chan, H. S., M. R. Wattenbarger, …, K. A. Dill. 1991. Enhanced structure in polymers at interfaces. *J. Chem. Phys.* 94:8542–8557.

35. Gupta, P., C. K. Hall, and A. Voegler. 1999. Computer simulation of competition between protein folding and aggregation. *Fluid Phase Equilib.* 158:87–93.

36. Zhou, H. X., and K. A. Dill. 2001. Stabilization of proteins in confined spaces. *Biochemistry.* 40:11289–11293.

37. Peterson, R. W., K. Anbalagan, …, A. J. Wand. 2004. Forced folding and structural analysis of metastable proteins. *J. Am. Chem. Soc.* 126:9498–9499.

38. Ravindra, R., S. Zhao, …, R. Winter. 2004. Protein encapsulation in mesoporous silicate: the effects of confinement on protein stability, hydration, and volumetric properties. *J. Am. Chem. Soc.* 126: 12224–12225.

39. Asuri, P., S. S. Karajanagi, …, R. S. Kane. 2007. Enhanced stability of enzymes adsorbed onto nanoparticles. *J. Nanosci. Nanotechnol.* 7:1675–1678.

40. Litt, J., C. Padala, …, R. S. Kane. 2009. Enhancing protein stability by adsorption onto raftlike lipid domains. *J. Am. Chem. Soc.* 131: 7107–7111.